Dynamic-finite-element and Dynamic-photoelastic Analyses of Two Fracturing Homalite-100 Plates

Numerically determined and experimentally established dynamic-energy-release rates show remarkable agreement with each other

by A. S. Kobayashi, A. F. Emery and S. Mall

ABSTRACT—A dynamic-finite-element code, HONDO, was used to analyze two single-edged-notch fracturing Homalite-100 plates which had been previously studied by dynamic photoelasticity. A single-edged crack in the finite-element model was advanced in incremental jumps such that the time-averaged crack velocity matched the measured crack velocity in the Homalite-100 plate. Dynamic-energy-release rates were computed for a constant-velocity crack and a crack which arrested after a somewhat constant deceleration. These results were compared with the corresponding dynamic-energy-release rates, which were computed from the dynamic-stress-intensity factors determined by dynamic photoelasticity, and with static-strain energy-release rates. Despite the crude modeling of the running crack, the coarseness of the finite-element-grid breakdown and the differences in the modeled and actual grip conditions, the computed and measured dynamic-energy-release rates, except for occasional large differences, generally agreed within 10 percent of each other.

Introduction

For the past six years, one of the authors and his colleagues[1-5] have been using dynamic photoelasticity to determine transient isochromatics in stiffened and unstiffened Homalite-100 plates with single-edged cracks subjected to uniaxial tension with and without impact loading under fixed grip conditions. More recently, dynamic photoelasticity was used to analyze the transient states in dynamic-tear-test (DTT) specimens and wedge-loaded double-cantilever-beam specimens. In the above dynamic-fracture experiments, the running cracks either arrested. branched and/or penetrated through the test specimens. In some instances, the running crack circumvented an open hole straight ahead in its path. In other cases, the crack would run through or arrest between pinned or pinned and bonded stringers which simulated riveted and riveted and adhesively bonded crack arresters. The dynamic photoelastic patterns in these tests were then used to determine dynamic-stress-intensity factors, dynamic-energy-release rates and crack velocities. The corresponding static-stress-intensity factors and static-strain energy-release rates were computed by using conventional finite-element analysis of a model with relatively coarse nodal breakdown. Average dynamic-energy-release rates, which are the total dynamic energies released during crack propagation divided by the total newly created crack-surface areas, were found to correlate with crack arrest and crack branching resulting in proposed crack arrest and crack-branching criteria.[6] A controversial conclusion derived through these investigations is that the arrest stress-intensity factor, unlike the critical stress-intensity factor, is not a material property as being proposed by some investigators.[7]

More recently, Dally *et al.* conducted dynamic-photoelasticity experiments to determine the fracture-dynamic parameters governing a running crack under static or dynamic loading.[8-10] The arrest stress-intensity factor in their investigation was found to be close to the critical stress-intensity factor and tends to verify the postulate that the arrest stress-intensity factor is a material property. In particular, their results agreed with the fracture-arrest concept advanced by Irwin in 1969.[11]

The above brief survey of the current and past investigations in fracture dynamics using dynamic photoelasticity show that different conclusions can be reached by different investigators possibly due to the differences in experimental setups and photoelastic models which they used. Such differences could imply certain fracture-dynamic parameters, such as the crack-arrest stress-intensity factor, should vary with

A. S. Kobayashi and A. F. Emery are Professors, and S. Mall is Graduate Student, University of Washington, Department of Mechanical Engineering, Seattle, WA 98195.

Paper was presented at 1976 SESA Spring Meeting held in Silver Spring, MD on May 9-14.

Original manuscript submitted: January 2, 1976. Revised version received: March 17, 1976.

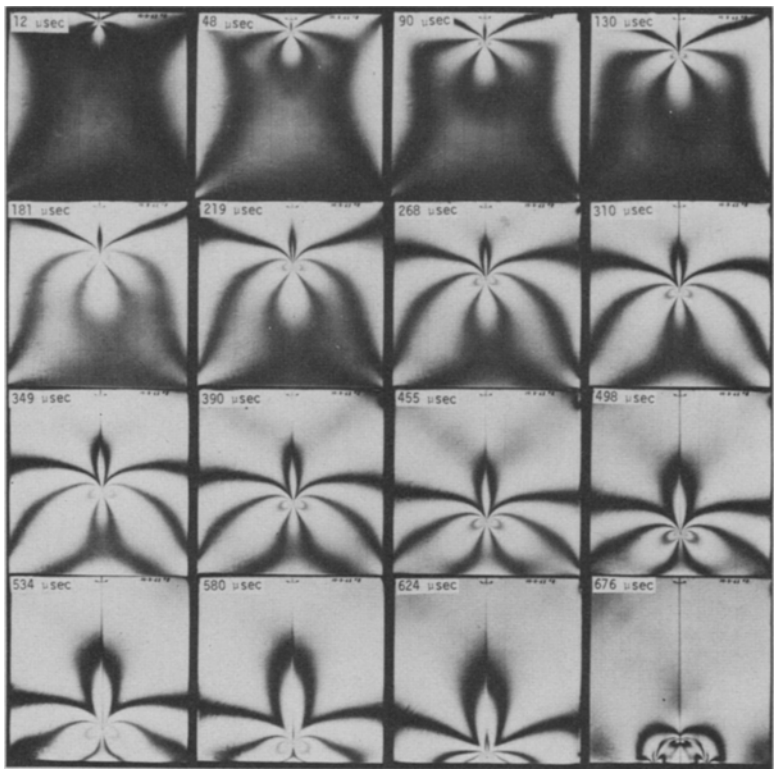

Fig. 1—Isochromatic patterns of dynamic crack propagation for Test No. B2

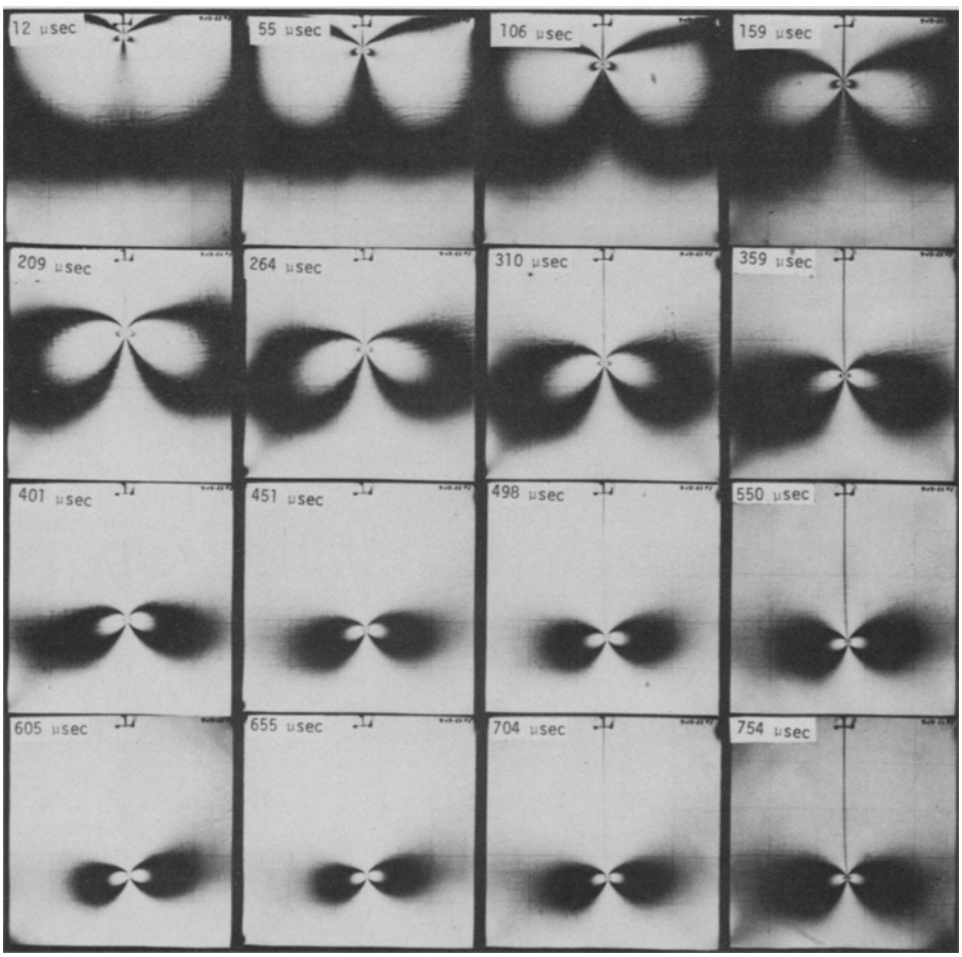

Fig. 2—Isochromatic patterns of dynamic crack propagation for Test No. B13

the solution procedure used if the dynamic-photoelasticity results, despite its numerous sources of experimental inaccuracies, yielded reasonably accurate dynamic-stress-intensity factors. At this time, when the authors felt that their dynamic-photoelasticity experiments should be re-examined independently by some other analytical, numerical or experimental procedure, the dynamic-finite-element code, HONDO, became available. This code was therefore used to simulate, as closely as possible, the fracturing Homalite plate such that the computed dynamic-fracture parameters could then be compared against those measured previously by dynamic photoelasticity. In the following, a brief account of this comparative study is given.

Dynamic-finite-element Code, HONDO

The dynamic-finite-element code, HONDO, used in this investigation was developed by S. W. Keys of the Sandia Laboratories.[12] It is a user-oriented finite-element code using explicit time-integration scheme and simple constant-strain quadrilateral elements. The code is capable of handling geometric nonlinearity as well as nonlinear material properties involving viscoplastic material and time-dependent boundary conditions.

Because the code is not capable of handling continuously extending cracks, the crack-tip motion was modeled by discontinuous jumps where the crack tip moved from one finite-element node to another at prescribed time intervals. The internodal distances divided by the time intervals of nodal jumps provided average crack velocities which were matched with the measured crack velocities in the fracturing Homalite-100 plate. This procedure was used with considerable success in previous work[13] but the jerky motion of the crack tip in the present analysis resulted in significant oscillations in the stresses and crack-opening displacements generated by the discrete burst of stress waves when the crack tip was advanced one nodal distance and the prescribed surface traction was suddenly applied to this newly freed crack surface. As a result, some time-averaging procedure was developed to extract dynamic-fracture information of a continuously running crack from the crack-tip model with intermittent jumps. Details of this procedure will be described in a following section.

Fracturing Homalite-100 Plates

Two previously reported dynamic-photoelasticity experiments involving ⅜-in.-thick Homalite-100 plates with uniform and linearly decreasing edge displacements[1] were re-analyzed by the dynamic-finite-element method. Figures 1 and 2 show the dynamic photoelastic patterns of this single-edge-cracked plate where the crack either propagated through the plate or arrested at approximately 70 percent of the plate width. Details of the procedure for computing the dynamic-stress-intensity factors are given in Ref. 1. In addition, the dynamic-energy-release rate was computed from the dynamic-stress-intensity factors by using Freund's equation.[14-16] Some detailed discussion on this computational procedure

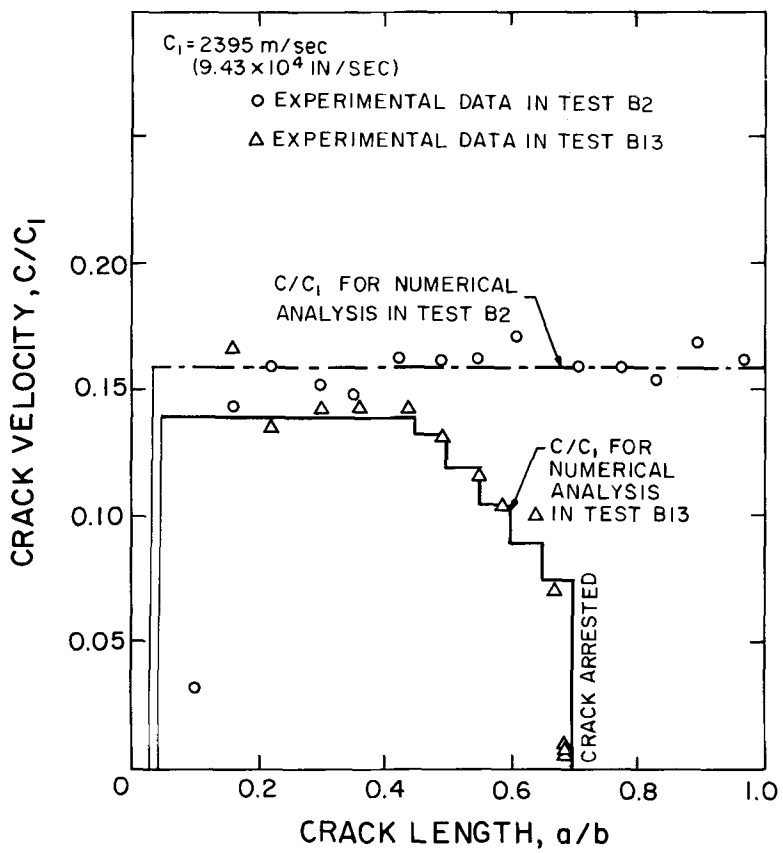

Fig. 3—Crack velocities in Test Nos. B2 and B13

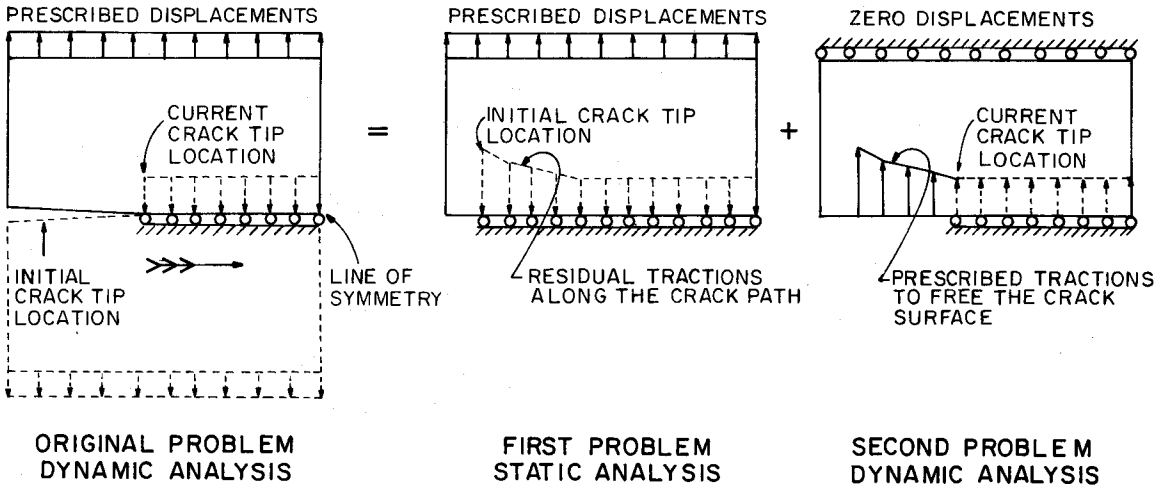

Fig. 4—Dynamic-finite-element analysis of a running crack in an edge-cracked tension plate subjected to prescribed displacement

is given in Ref. 5. The generality of Freund's equation relating the dynamic-energy-release rate and the dynamic-stress-intensity factor is also described in Ref. 17.

In the past, crack velocities measured directly from the dynamic photoelastic pictures and the Lite-Mike timing marks were faithfully recorded as instantaneous crack velocities which were shown to fluctuate as the crack propagated. More-accurate crack-velocity measurements by Döll[18] who showed that the crack velocity does not change even under the severe condition of crack branching indicate that the fluctuation in the recorded crack velocities may be an artifact of the experimental procedure. As a result, the small fluctuations in apparent crack velocities are ignored and smoothed crack velocities, shown in Fig. 3, were assigned as input conditions to the finite-element analysis of the two Homalite-100 plate specimens.

The averaged dynamic material properties of Homalite-100 plates used here were determined by Bradley.[1] The dynamic modulus of elasticity, dynamic Poisson's ratio, dynamic-stress-optic coefficient and static-fracture toughness are 4.65 GPA (675 psi), 0.345, 27.1 kPa-m/fringe (155 psi-in./fringe) and 636 kPa$\sqrt{m}$ (579 psi $\sqrt{in.}$), respectively.

Dynamic-finite-element Analysis of the Fracturing Homalite-100 Plates

As described previously, the essential feature of this finite-element analysis is in propagating the crack at prescribed crack velocities which were determined experimentally from previous dynamic photo-

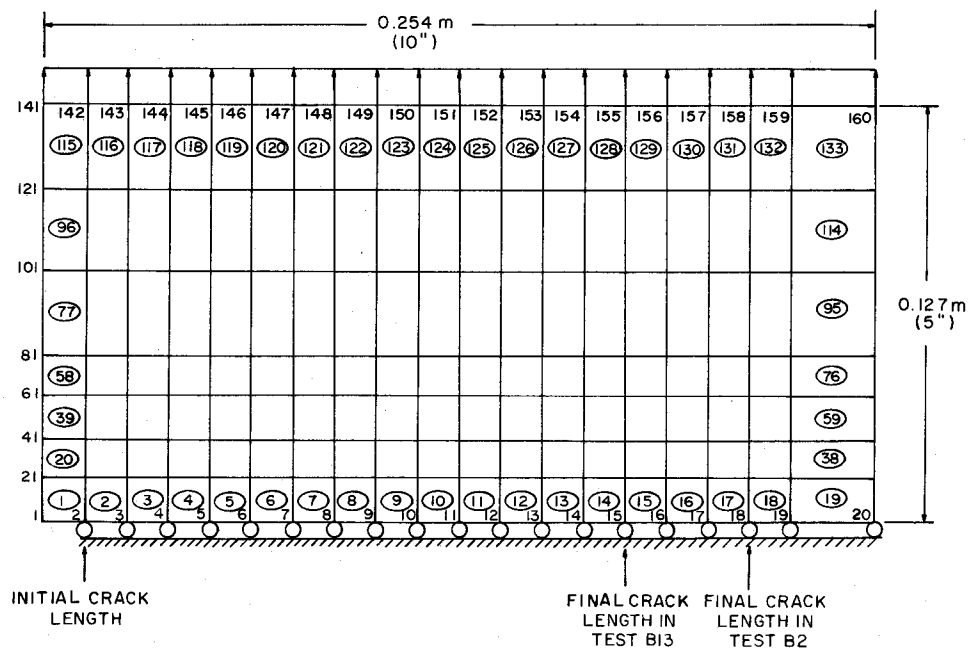

Fig. 5—Finite-element breakdown of an edge-cracked tension plate

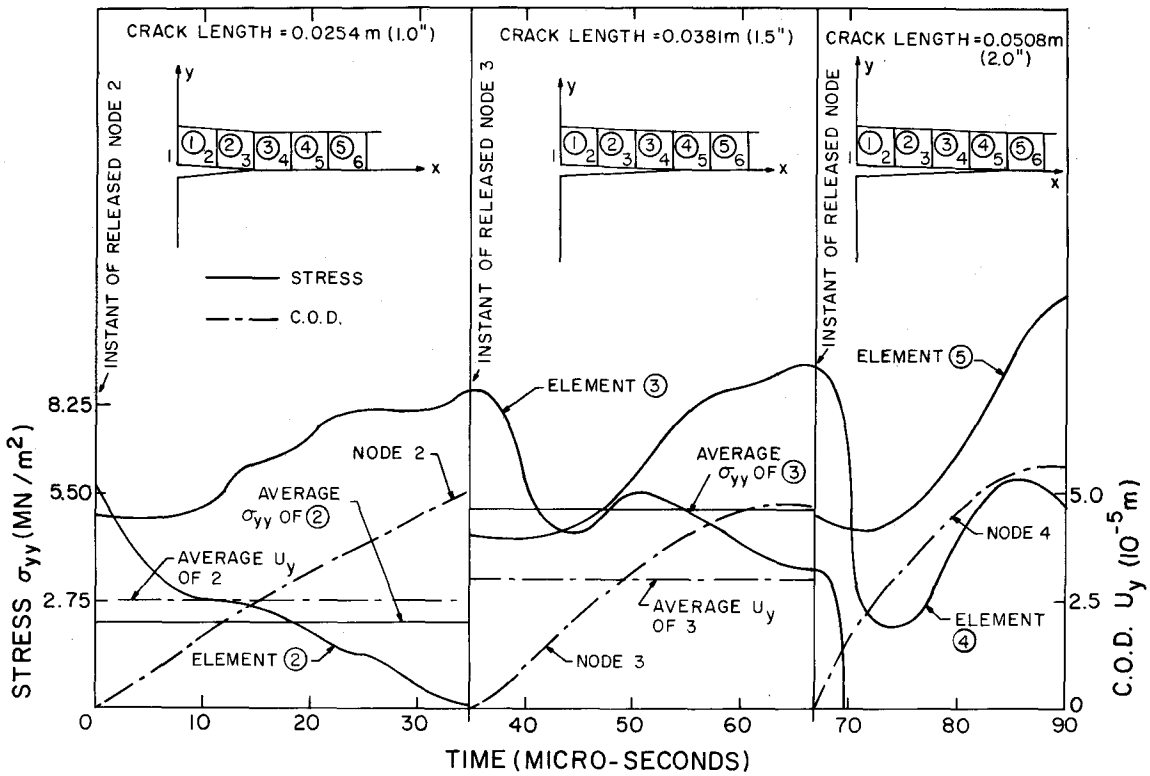

Fig. 6—Stresses ahead and behind the crack tip and C.O.D. of running crack in Test No. B2

elastic analysis. The computed dynamic states of stress, strain and dynamic crack-opening displacements (COD) are then sifted for possible clues for a dynamic fracture and crack-arrest criterion. This procedure differs from those used in Refs. 13 or 19 where the crack propagates under hypothetical dynamical-fracture criteria.

The actual dynamic-finite-element solution consisted of superposition of two solutions, namely a static solution of the initial single-edged cracked plate under fixed-grip loading and a fracturing plate with an unloaded fixed-grip plate with surface tractions prescribed over the crack surface shared by the side of a finite element which has just been freed by a discrete jump in the crack-tip node. Figure 4 shows schematically this fracturing plate. By superposing a succession of dynamic solutions with increasing crack lengths to the static solution of the first problem, the dynamic solution to the original problem is obtained for a given time or crack length modeled by the superposition of these two solutions.

Figure 5 shows the finite-element breakdown used in this investigation. Only half of the specimen is considered because of symmetry of the problem and thus a total of 133 elements and 160 nodes were used. The fixed-gripped condition is simulated by prescribed normal displacements with vanishing tangential tractions. For simplicity in modeling, the initial crack length in the two problems were assumed to be of 0.0127 m (0.5 in.).

Solutions to the first problem, which are two static analyses of two Homalite-100 plate specimens with prescribed boundary displacements of uniform or linearly decreasing boundary displacements, were obtained by using a standard static-finite-element program with quadrilateral elements. Total CPU time on a CDC 6400 computer for such analysis is typically 57 s.

Identical finite-element breakdown was used in the second problem with prescribed vanishing-boundary displacements on the gripped edges of the specimen. As mentioned earlier, crack propagation was accomplished by freeing the current crack-tip node at discrete time intervals. Simultaneously, a normal surface traction, which is equal in magnitude and opposite in sign with the residual normal surface traction at corresponding location in the static solution, is prescribed on the crack side of the rectangular element containing the newly freed node and the new crack-tip node. These surface tractions remain prescribed during the entire crack-propagation interval.

Because of the discontinuous advance of the crack tip, the normal stresses in elements surrounding the old and new crack tip as well as the crack-opening displacements (COD) in the second problem showed significant oscillations. The relative magnitudes of such oscillations in the resultant stresses and resultant COD are shown in Fig. 6. Also shown are time averages of these quantities which were then used to estimate the dynamic-stress-intensity factor, K_D. Inherent numerical errors in K_D estimations due to the coarse nodal breakdown were somewhat reduced by scaling the K_D with the ratio of a static-stress-intensity factor obtained from coarse-grid analysis. These K_D values were then used to compute the dynamic-energy-release rate, $\mathcal{G}_D$, using Freund's equation[14-16] with the known crack-velocity curve in Fig. 2. The total dynamic energy released which was obtained by

integrating the area under this $\mathcal{G}_D$ must be at the most equal or less than the total energy released which is determined from the corresponding curve of static-strain energy-release rate, $\mathcal{G}$. The total dynamic energy determined from stress consideration was 1.02 times the latter total static-strain energy in Test B2 and is a physical impossibility. When the dynamic COD was used to compute the total dynamic energy released, this value was 0.86 of the total static-strain energy released and is much higher than the corresponding ratio of 0.69 obtained from dynamic photoelasticity. This comparison indicated that K_D determined both from local stresses or local COD could be over-estimated, possibly as much as 20-30 percent, when one considers the possible dynamic energy losses in the test specimens.

In order to reduce the induced numerical errors due mainly to the coarseness of the finite-element breakdown, a direct procedure of computing the dynamic energy released, which follows the static procedure, was used. For the time-averaged stress and time-averaged COD, during the increment of crack advance, Δt, the dynamic energy released in this element algorithm becomes,

$$\Delta E = 2[\sigma_{yy}]_{\text{ave}} \cdot [u_y]_{\text{ave}} \, \Delta a \qquad (1)$$

where

Δa is the incremental advancement of the crack tip and is equal to length of the side of the rectangular element sharing the crack-tip node.

$[\sigma_{yy}]_{\text{ave}}$ is the time-averaged stress in this element during the time increment prior to crack advance.

$[u_y]_{\text{ave}}$ is the time-averaged COD of the freed node on the crack surface in this element during the time increment after crack advance.

The dynamic-stress-intensity factor can be computed by Freund's formula[13] of,

$$K_{ID} = \left\{ 2G \cdot \frac{\Delta E}{\Delta a} \frac{(1+\beta_2^2)^2 - 4\beta_1\beta_2}{\beta_1(\beta_2^2 - 1)} \right\}^{1/2} \qquad (2)$$

where

G is the dynamic shear modulus of Homalite-100

$$\beta_1^2 = 1 - \left(\frac{C}{C_p}\right)^2$$

$$\beta_2^2 = 1 - \left(\frac{C}{C_2}\right)^2$$

C is the crack velocity

C_p is the plate velocity in Homalite-100

C_2 is the distortional wave velocity in Homalite-100

Because of the algorithm used in computing the dynamic energy released during crack propagation, this dynamic-stress-intensity factor is assigned to the new crack-tip node after crack advance.

The accuracy of this direct computational procedure for dynamic-energy-release rate was assessed by modeling Baker's solution[20] (plane strain) which was also studied in some detail by G. C. Smith.[21] For this purpose, the same finite-element model shown in Fig. 5 with an initial crack length of 0.1143 m (4.5 in.) and zero boundary displacement was used. This problem can be considered as a semi-infinite crack in an infinite plate (plane strain) if the reflected stress waves do not reach the region of the moving crack tip or, for this particular problem, if the lapse time is less than approximately 80 μs. A unit pressure was applied at $t = 0^+$ and the crack was advanced 0.0127 m (0.5 in.) twice at $t = 31.5$ and 67.5 μs. The dynamic-stress-intensity factor at 31.5 μs for a stationary crack in a Homalite-100 plate, suddenly pressurized by 36.9 Pa (1 psi) is,[20]

$$K_s\,(t = 31.5\text{ s}) = 1.677\text{ kPa}\sqrt{\text{m}}\ (1.527\text{ psi}\sqrt{\text{in.}})$$

The dynamic-stress-intensity factor for a pressurized crack running at a crack velocity of $C = 4030$ m/s (1.59×10^4 in./s) can be computed by[14] as,

$$K_{ID} = k(C) \cdot K_s\,(t = 31.5\,\mu\text{s})$$

$$= 1.37\text{ kPa}\sqrt{\text{m}}\ (1.25\text{ psi}\sqrt{\text{in.}})$$

where the value of function, $k(C) = 0.8$, was read off from Fig. 3 in Ref. 14.* The dynamic-stress-intensity factor obtained from the dynamic-energy-release rate (plane strain) computed directly by the HONDO analysis is 1.35 kPa $\sqrt{\text{m}}$ (1.24 psi $\sqrt{\text{in.}}$) which is in excellent agreement with the analytical results.

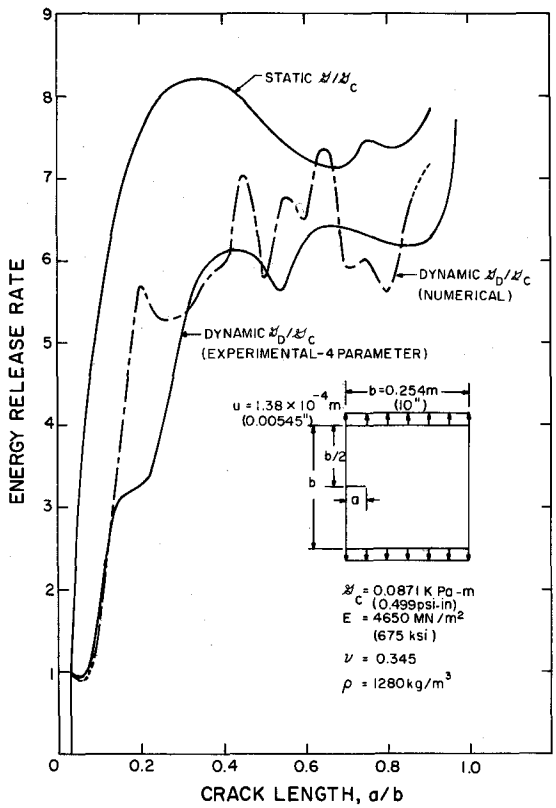

Fig. 7—Energy-release rates (plane stress) in Test No. B2

* *Figure 3 in Ref. 14 was constructed for a material with Poisson's ratio of 0.25 and not 0.345 of Homalite-100. The error due to this difference in Poisson's ratio is estimated to be about 1 percent from Ref. 22.*

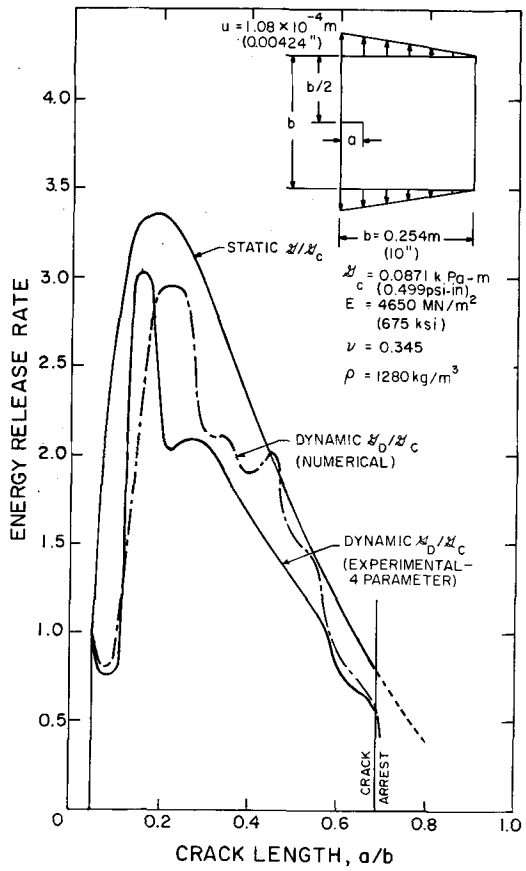

Fig. 8—Energy-release rates (plane stress) in Test No. B13

Results

Using the finite-element model shown in Fig. 5, the initial crack of length 0.0127 m (0.5 in.) was advanced in 16 increments to a crack length of 0.2159 m (8.5 in.) at appropriate time intervals. The total CPU time of a CDC 6400 computer for such analysis is typically 345 s.

The dynamic-energy-release rate, (plane stress), $\mathcal{G}_D = \Delta E/\Delta a$, obtained directly by the procedure described above, are plotted in Figs. 7 and 8 for the constant-velocity crack in Test B2 and the arrested crack in Test B13. These dynamic-energy-release rates are normalized by the critical-strain energy-release rate, $\mathcal{G}_c$, of the Homalite-100 plate. Also shown in these figures are the corresponding static-strain energy-release rate, (plane stress), $\mathcal{G}$, and the dynamic-energy-release rate, (plane stress), $\mathcal{G}_D$, determined directly from the dynamic-stress-intensity factor, K_D, obtained via dynamic photoelasticity using the method of four parameter fitting of isochromatics.[1] Other than the differences in the detailed maximum and minimum values, the agreements between the experimental and numerical $\mathcal{G}_D$ values are remarkable.

The total energies released by the numerical and experimental $\mathcal{G}_D$ curves in Test B2 are 75 percent and 72 percent, respectively, of the total static-strain energy released. This agreement is remarkable when one considers the differences in boundary conditions between the numerical and experimental models of the fracturing Homalite-100 plate. For Test B13, the total energies released by the numerical and experimental $\mathcal{G}_D$ curves are 77 percent and 68 percent, respectively, of the total static-strain energy released.

Discussion

It is interesting to note that the dynamic-finite-element results as well as a re-examination of the old dynamic-photoelasticity results show momentary decreases in dynamic-energy-release rate immediately after the initiation of crack propagation in Figs. 7 and 8. Such dip at a lower crack velocity has been postulated by Irwin[23] and has been used by Kanninen in his crack-propagation model.[24]

Figure 8 shows that the numerically determined dynamic-energy-release rate, $\mathcal{G}_D$, prior to crack arrest was almost identical to its experimental counterpart and is less than 75 percent of the corresponding static-strain energy-release rate at the arrest-crack length. The numerically determined dynamic-energy-release rate at arrest coincides with its experimental counterpart and is about 0.51 $\mathcal{G}_c$ but then drops further to about 0.4 $\mathcal{G}_c$ immediately after arrest. This good agreement between the experimental and numerical arrest values of the dynamic-energy-release rate underscores the importance of reanalyzing, by this dynamic-finite-element procedure, our previous crack-arrest experiments which yielded unexpectedly low arrest stress-intensity factors[1,2,5] which also varied with test-specimen configurations. The latter finding implies the inadequacy in using static equivalency in determining an arrest stress-intensity factor as a material property.

The numerical result for the crack-arrest case yields an average dynamic-energy-release rate of $\mathcal{G}_D]_{ave} = 1.66\ \mathcal{G}_c$ at arrest. This large $\mathcal{G}_D]_{ave}$ at crack arrest is due to the lack of dissipated energies, which are of significant magnitude in our dynamic-photoelasticity experiments.

The effect of the differences in the boundary conditions prescribed in the finite-element model and the dynamic photoelastic model has been of general concern since the inception of this finite-element analysis. These differences are indicated in the plots of maximum shear stresses at four locations along the specimen boundary with time. Other than the lack of stress singularity at the specimen corner in the finite-element model the differences in the stress-boundary conditions of the finite-element model and the dynamic-photoelasticity model was smaller than expected. Thus, the edge-boundary conditions prescribed in the finite-element model appear to be a fair modeling of the actual boundary conditions in the dynamic-photoelasticity experiments.

Conclusions

A simple dynamic-finite-element program has been used to successfully model two fracturing Homalite-100 plates in which the crack propagated through at a constant velocity in one case and arrested in the second case. The numerically determined and experimentally established dynamic-energy-release rates showed remarkable agreement with each other. With appropriate development, two-dimensional dynamic-finite-element analysis should be replacing two-dimensional dynamic photoelasticity in its ap-

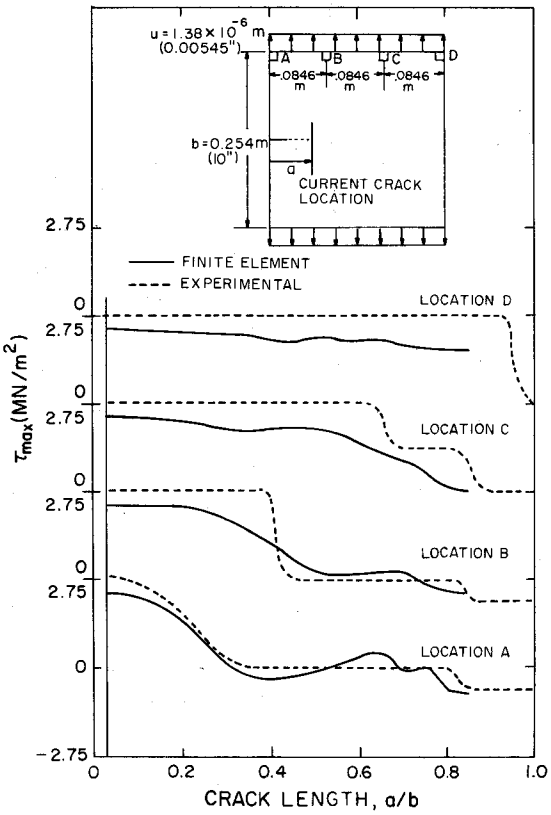

Fig. 9—Maximum shear stress at different locations along specimen boundary in Test No. B2

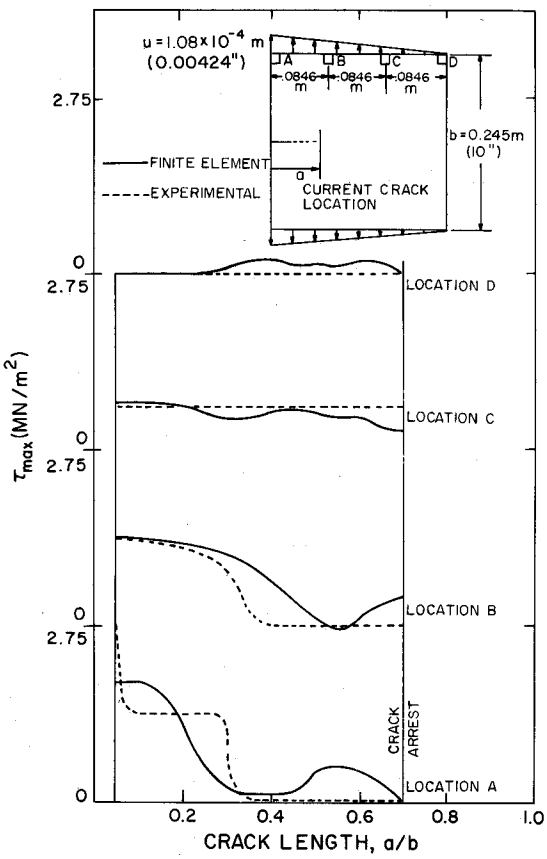

Fig. 10—Maximum shear stress at different locations along specimen boundary in Test No. B13

plication to fracture dynamics in the near future.

Acknowledgment

The results in this investigation were obtained in a research contract funded by the Office of Naval Research under Contract No. N00014-76-C-0060, NR 064-478. The authors wish to acknowledge the support and encouragement by N. R. Perrone and H. Basdegas of ONR.

References

1. Bradley, W. B. and Kobayashi, A. S., "Fracture Dynamics—a Photoelastic Investigation," Engrg. Fract. Mech., 3, 317-332 (1971).

2. Kobayashi, A. S., Wade, B. G. and Bradley, W. B., "Fracture Dynamics of Homalite-100," Deformation and Fracture of High Polymers (ed. by H. H. Kausch, J. A. Hassell and R. I. Jaffee) Plenum Press, New York, 487-500 (1973).

3. Kobayashi, A. S. and Wade, B. G., "Crack Propagation and Arrest in Impacted Plates," Dynamic Crack Propagation (ed. by G. C. Sih), Noordhoff International, 663-677 (1973).

4. Kobayashi, A. S. and Chan, C. F., "A Dynamic Photoelastic Analysis of Dynamic-tear-test Specimen," EXPERIMENTAL MECHANICS, 16 (5), 176-181 (May, 1976).

5. Kobayashi, A. S., Mall, S. and Lee, M. H., "Fracture Dynamics of Wedge-Loaded DCB Specimen," to be published in the Proc. of the Ninth National Symposium on Fracture Mechanics (1975), ASTM STP.

6. Kobayashi, A. S., Mall, S. and Bradley, W. B., "A Dynamic Photoelastic Analysis of Crack Branching," Proc. of 12th Annual Meeting of the Society of Engineering Sciences, Univ. of Texas at Austin, 1005-1014 (Oct. 1975).

7. Crosley, P. B. and Ripling, E. J., "Plane Strain Crack Arrest Characteristics of Steels," ASME Paper No. 75-PVP-32. To be published in the J. of Pressure Vessel Technology, Trans. of ASME.

8. Dally, J. W., Fourney, W. L. and Holloway, D. C., "Stress Wave and Fracture Propagation from a Continued Explosive Charge Near a Free Boundary," Proc. of the 12th Annual Meeting of the Society of Engineering Sciences, Univ. of Texas at Austin, 1257-1270 (Oct. 1975).

9. Kobayashi, T. and Fourney, W. L., "Dynamic Photoelastic Investigation of Crack Propagation," ibid loc cit., 131-140.

10. Fourney, W. L., Holloway, D. C. and Dally, J. W., "Fracture Initiation and Propagation from a Center of Dilatation," Intnl. J. of Fracture, 11 (6), 1011-1029 (Dec. 1975).

11. Irwin, G. R., "Basic Concept for Dynamic Fracture Testing," J. of Basic Engineering, Trans. of ASME, 91 Series D, 519-524 (Sept. 1969).

12. Keys, S. W., "HONDO—A Finite Element Computer Program for the Large Deformation Dynamic Response of Axisymmetric Solids," Sandia Laboratories Rep. SLA-74-0039 (April 1974).

13. Emery, A. F., Love, W. J. and Kobayashi, A. S., "Elastic Crack Propagation Along a Pressurized Pipe," J. of Pressure Vessel Technology, Trans. of ASME, 98 Series J, (1), 2-7 (Feb. 1976).

14. Freund, L. B., "Crack Propagation in an Elastic Solid Subjected to General Loading—I, Constant Rate of Extension," J. of the Mech. and Phys. of Solids, 20, 129-140 (1972).

15. Freund, L. B., "Crack Propagation in an Elastic Solid Subjected to General Loading—II, Non-Uniform Rate of Extension," ibid loc cit., 141-152.

16. Freund, L. B., "Crack Propagation in an Elastic Solid Subjected to General Loading—III, Stress Wave Loading," J. of the Mech. and Phys. of Solids, 21, 47-61 (1973).

17. Nilsson, F., "A Note on the Stress Singularity at a Non-Uniformly Moving Crack Tip," J. of Elasticity, 4 (1), 73-75 (Mar. 1974).

18. Döll, W., "Investigation of the Crack Branching Energy," Intnl. J. of Fracture, 11, 184-186 (1975).

19. Kanninen, M. F., "A Dynamic Analysis of Unstable Crack Propagation and Arrest in DCB Test Specimen," Intnl. J. of Fracture, 10 (3), 415-430 (Sept. 1974).

20. Baker, B. R., "Dynamic Stresses Created by a Moving Crack," J. of Ap. Mech., Trans. of ASME, 29 Series E, (3), 449-458 (Sept. 1962).

21. Smith, G. C., "An Experimental Investigation of the Dynamic Fracture of a Brittle Material," a PhD Thesis submitted to California Institute of Technology (April 15, 1975).

22. Clifton, R. J., "Some Recent Developments in Fracture Mechanics," Terra Tek, Salt Lake City, Utah (Nov. 13, 1974).

23. Irwin, G. R., Private communication, June 1975.

24. Hoagland, R. G., Rosenfield, A. R., Kanninen, M. F. and Hahn, G. T., "Rectangular DCB Specimens for Fast Fracture and Crack Arrest Measurements," Battelle Columbus Laboratory Rep. BM1-1973, Columbus, OH (Dec. 1974).

25. "Criteria for Crack Branching and Crack Arrest," Prog. in Experimental Mechanics—Durelli Anniversary Volume (ed. by V. J. Parks) Catholic University of America, 83-97 (1975).